Contents

Chapter 1

Introduction

Initially after the Big Bang, there were one billion and one matter particles for one billion anti-matter particles, which suggests that the current universe should also have abundant anti-matter. However, our current universe is almost entirely built up by matter particles. This is famously known as matter-antimatter asymmetry and is one of the open questions of physics. A fundamental difference in the behavior of matter and antimatter, the *CP* violation, is one of the effects known as Sakharov conditions to explain this asymmetry.

The *CP* symmetry is the product of two symmetries: the charge inversion *C*, which describes the transition of particles into their antiparticles, and the space coordinate mirroring parity *P*. In 1973, Kobayashi and Maskawa introduced a mechanism to explain *CP* violation in the Standard Model (SM) through the CKM matrix - a mathematical framework describing how quarks change flavors via the weak force.

Despite its success, the *CP* violation predicted by the Standard Model is far too small to explain the vast matter-antimatter imbalance. Therefore, new sources of *CP* violation are needed and many New Physics models propose them. Searching for deviations from SM predictions in precision experiments could reveal such new physics and perhaps even explain other open questions, like dark matter.

The *CP* violation can be studied experimentally by comparing the decays of particles and antiparticles. The LHCb experiment is specifically designed for such studies in the B meson region and has already provided substantial results. The analysis to be performed in this study is based on the largest *CP* violation effects observed on the Run 1 dataset.

This analysis is performed on a dataset of reconstructed events of B decays and the objective is to compare the decay rates of $B^+ \to h^+h^+h^-$ and the ones of its antiparticle equivalent $B^- \to h^-h^-h^+$, where $h^\pm$ can be pions ($\pi^\pm$) or kaons ($K^\pm$). The possible decays are:

- $B^+ \to K^+K^+K^-$
- $B^+ \to \pi^+K^+K^-$
- $B^+ \to K^+\pi^+\pi^-$

- $B^+ \to \pi^+\pi^+\pi^-$

as well as their corresponding antiparticle decays. Due to the low background level this analysis focuses on the $B^+ \to K^+K^+K^-$ decay. In order to recognize and select only events involving B decays, some important physical properties such as momentum, mass and impact parameter are considered. Figure 1-1 shows Feynman diagrams for the $B^+ \to K^+K^+K^-$ decay.

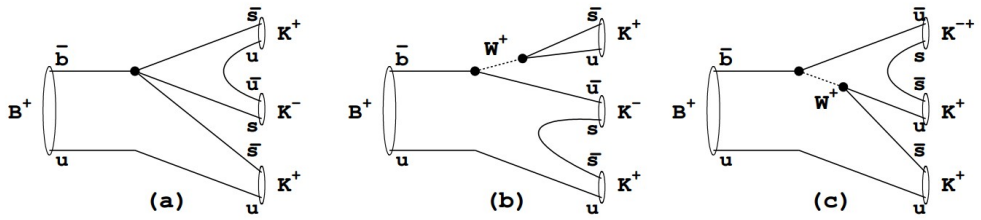

Figure 1-1: Feynman diagrams for $B^+ \to K^+K^+K^-$ decay: (a) b $\to$ s penguin; (b) and (c) b $\to$ u trees [1].

Chapter 2

LHCb

The Large Hadron Collider (LHC) is a particle accelerator at CERN, the European organization for nuclear research, close to Geneva and LHCb is one of the four main experiments at the LHC. The data used in this analysis was taken during Run 1 of the pp collision with 7 TeV center-of-mass energy but filtered through different triggering techniques. The schematic diagram of the LHCb is shown in Figure 2-1.

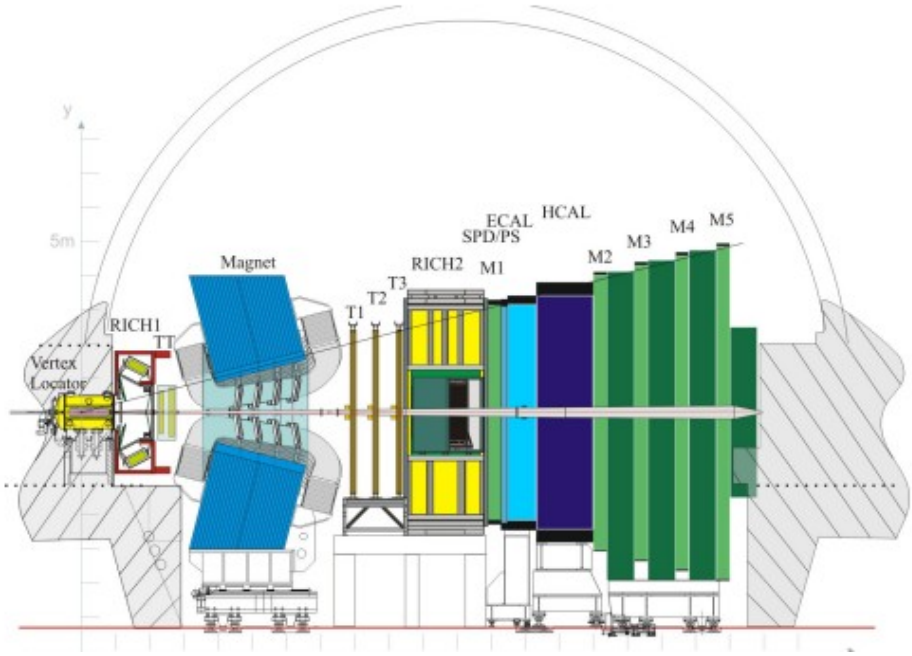

Figure 2-1: Schematic diagram of the LHCb detector.

Unlike the large, symmetric detectors like ATLAS and CMS, LHCb has a forward geometry, focusing on particles emitted at small angles relative to the beam line, where b-hadrons are most frequently produced. The detector is a forward spectrometer, about 20 meters long, consisting of several specialized components arranged in a sequence. Closest to the collision point is the Vertex Locator (VELO), which uses high-precision silicon sensors to detect where

particles originate and helps distinguish the decay vertices of short-lived particles. Following VELO is the tracking system, which measures the momentum of charged particles as they curve in a magnetic field provided by a large dipole magnet.

To identify the type of each particle, LHCb uses two RICH (Ring Imaging Cherenkov) detectors that detect light emitted when charged particles travel faster than the speed of light in a medium. These detectors help distinguish between similar particles like pions, kaons, and protons. Further along the detector are the electromagnetic and hadronic calorimeters, which measure the energy of electrons, photons, and hadrons by absorbing them. At the far end is the muon detection system, which identifies muons that pass through all other layers of the detector, as muons are crucial in identifying many rare decay processes. LHCb also features a sophisticated trigger system, which quickly filters out the vast majority of uninteresting collisions and keeps only the events likely to contain b-hadrons or other particles of interest. The combination of precision vertex detection, excellent momentum measurement, and robust particle identification makes LHCb exceptionally capable of studying rare decays, CP violation, and potential signs of new physics beyond the Standard Model. Two of the key uses of the LHCb detector is to study of matter-antimatter asymmetry and rare decays of b- and c-quarks.

Chapter 3

Results and Analysis

The purpose of the experiment is to analyze the decay rates $B^+ \to K^+K^+K^-$ and its antiparticle equivalent $B^- \to K^-K^-K^+$ to observe CP violation both globally and locally.

3.1 B^+ and B^- decays from Simulation

The study is based on the investigation of simulations of B^+ and B^- decay results. Figure 3-1 shows the histogram of the momentum components of the three candidate kaon. It is clearly observed that in the z-direction, the momentum increases while the number of events decreases exponentially. In contrast, the x- and y-momentum distributions follow normal distributions with means of 0.85 MeV/c and 47.98 MeV/c, respectively.

The histograms of the momentum components in the X and Y directions follow a Gaussian distribution indicating symmetry in those directions. Meanwhile, The Z component of momentum appears asymmetric because the colliding partons have unequal momentum fractions causing a boost along Z.

The results of the energy computed using Equation 3.1 are shown in Figure3-3. The energy and momentum distributions of the three kaon candidates appear very similar in both shape and trend which supports the conclusion that the candidates are particle–antiparticle pairs of each other. Moreover, collisions between partons are less frequent at higher energies, which leads to an exponential-like decrease in the energy distribution.

From the Einstein energy-mass relation and the conservation of energy and momentum combined with the well-known value of the kaon mass $m_K \approx 493.7\,\mathrm{MeV}/c^2$, the mass of a $B^\pm$ meson candidate can be calculated using the following equation:

$$E = \sqrt{p^2c^2 + m^2c^4} \tag{3.1}$$

where E is the energy of the hadron, p is its momentum computed using Equation 3.2, m is a mass of $B^\pm$ meson candidate, and c is the speed of light (here, $c = 1$).

The total momentum P of a candidate is calculated using its components along the x-, y-, and z-axes as follows:

$$P = \sqrt{P_x^2 + P_y^2 + P_z^2} \tag{3.2}$$

The mass distribution of the $B^{\pm}$ meson candidates is shown in Figure 3-2. The peak of the histogram is at 5267.43 MeV/c^2.

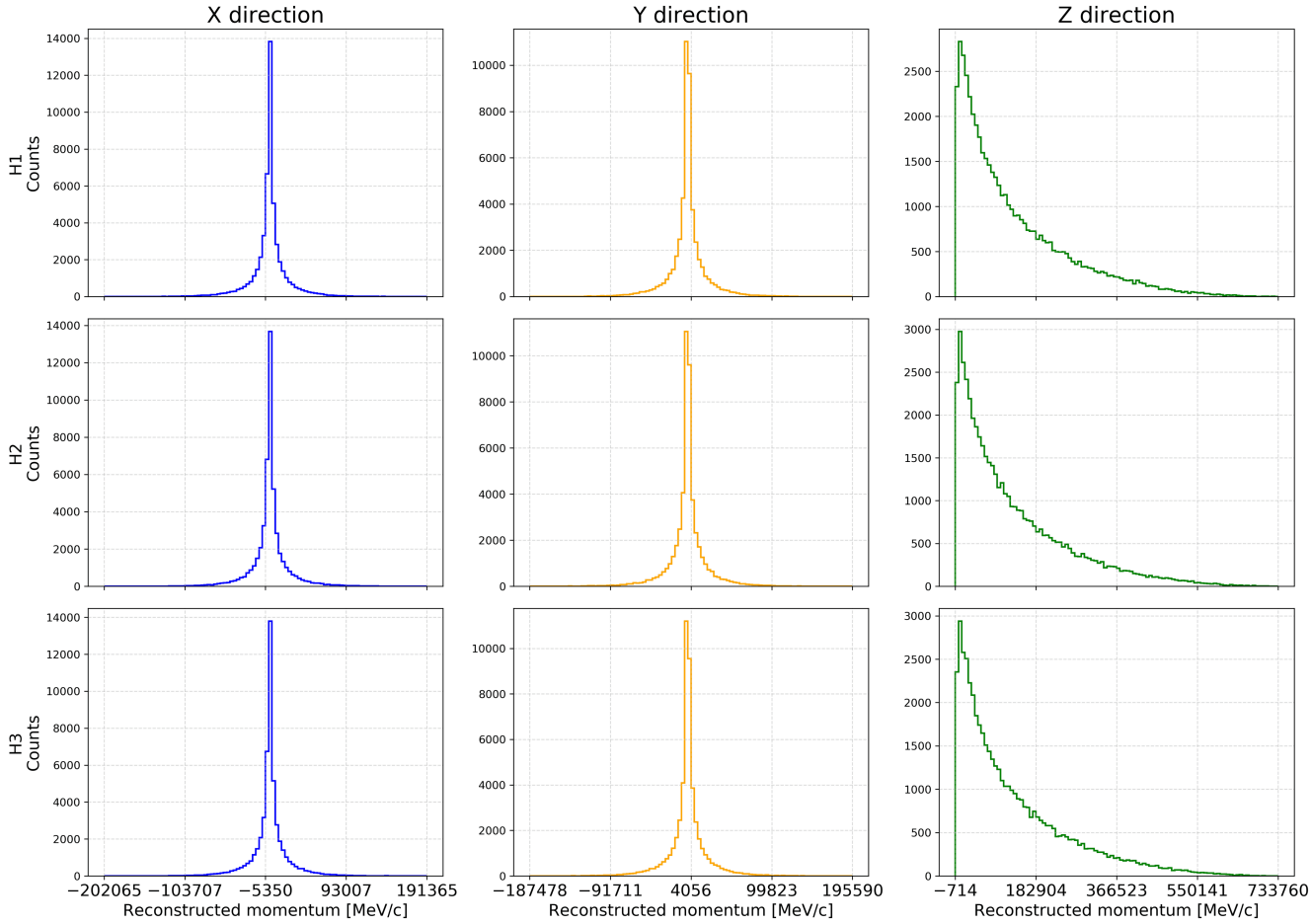

Figure 3-1: Histogram of the momentum components of the three candidate kaons H_1, H_2, and H_3. The x- and y-components are perpendicular to the beam z-axis.

Thus, the simulation appears reasonable and the results provide a hint for further investigation in the experimental data.

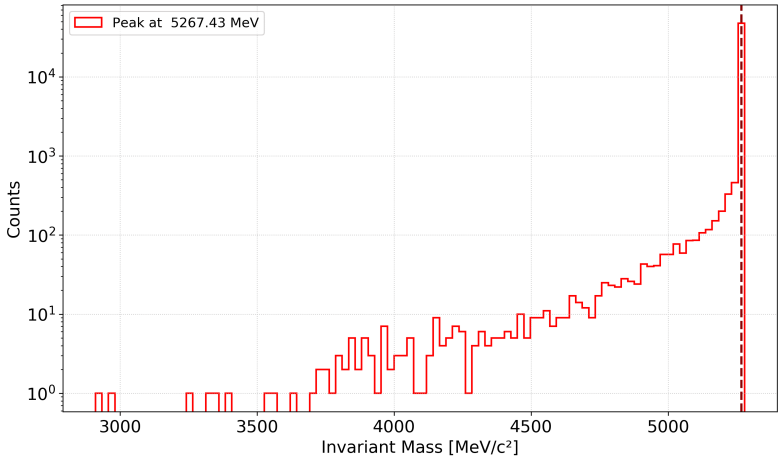

Figure 3-2: Histogram of the mass of $B^{\pm}$ meson candidate.

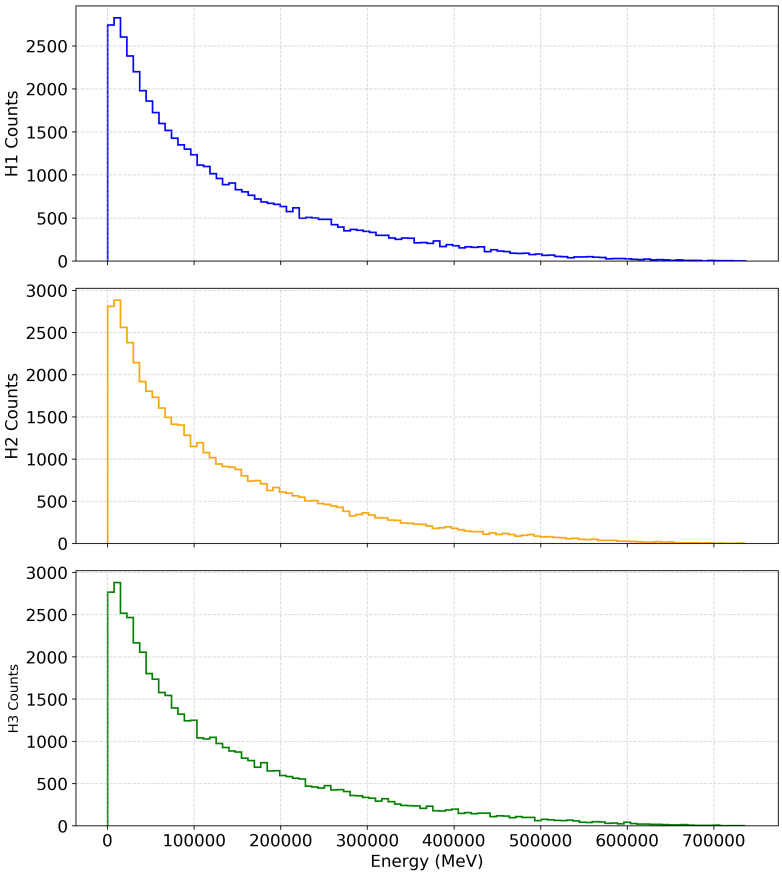

Figure 3-3: Histogram of the energy of the three candidate kaons.

3.2 B^+ and B^- decays from LHCb

To analyze LHCb experimental data, a preselection procedure is essential to reduce the combinatorial background and improve the signal-to-noise ratio. This analysis was performed by applying the following criteria in Table 3.1. Figure 3-4 illustrates the probability distributions after applying the selection criteria.

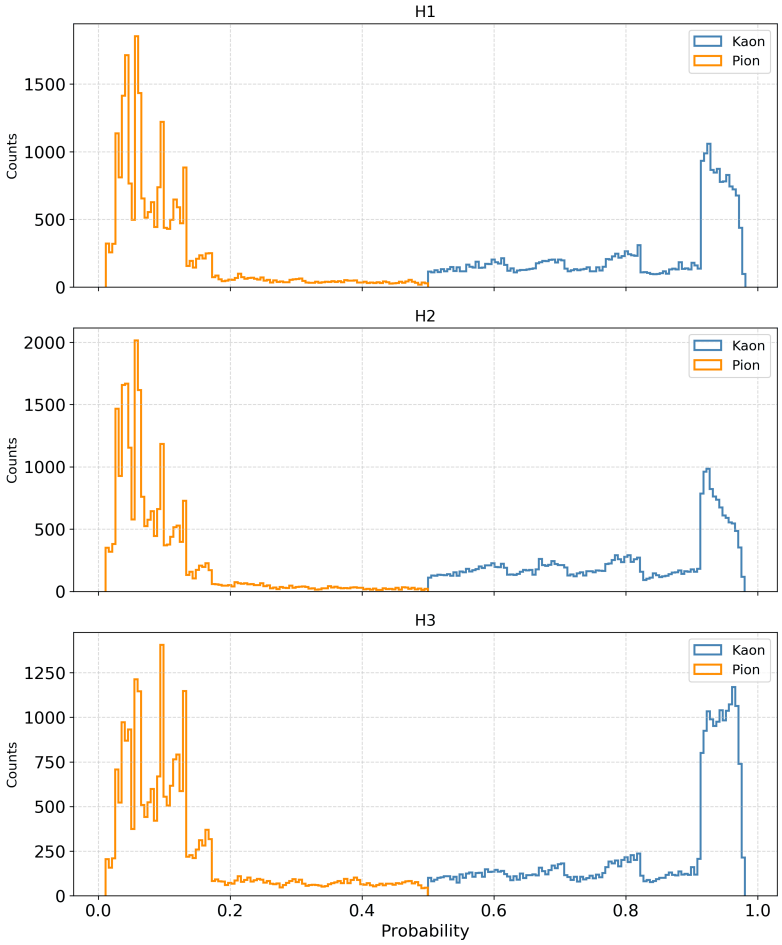

Figure 3-4: Probability distribution of candidate kaons and Pions.

The selection also ensures that muons are excluded. Following the procedure to calculate the mass of the $B^{\pm}$ boson (see Equation 3.1), the results are shown in Figure 3-5. The mass peak at 5281.24 MeV/c^2. compared to the simulated data peak at 5267.43 MeV/c^2 is quite close and within reasonable agreement. The shape of the LHCb data clearly shows the challenges of measurement and simulation, including detector resolution effects and background contributions, as seen in Figure 3-5.

Table 3.1: Preselection criteria applied to candidate kaons in the analysis.

Criterion	**H1**	**H2**	**H3**
isMuon	0	0	0
Probability of being a pion	< 0.5	< 0.5	< 0.5
Probability of being a kaon	> 0.5	> 0.5	> 0.5

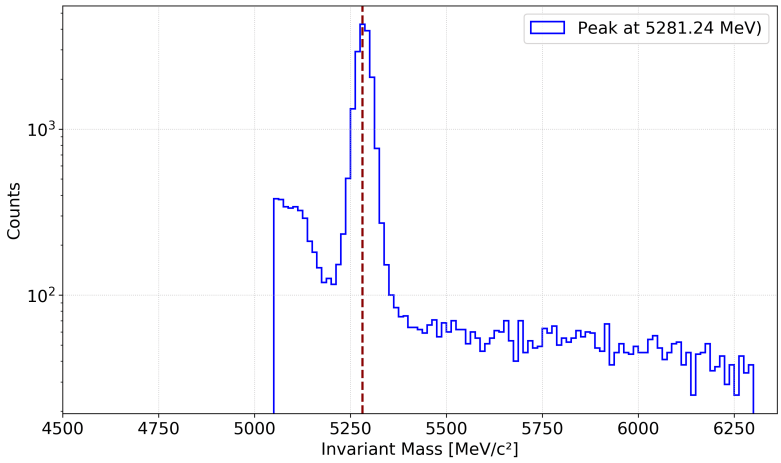

Figure 3-5: Histogram of the mass of $B^{\pm}$ meson candidate from LHCb experiment.

3.3 Global CP violation

To investigate CP violation, the $B^{\pm}$ meson candidates are separated based on the charge conservation of the three kaon candidate decay products, $B^+ \to K^+K^+K^-$ and $B^- \to K^-K^-K^+$. To search for global matter–antimatter asymmetry, the following equation is used to determine the asymmetry:

$$A = \frac{N^+ - N^-}{N^+ + N^-} \tag{3.3}$$

where N^+ and N^- represent the number of B^+ and B^- candidates, respectively.

However, the observed asymmetry may not arise from CP violation. It can also include contributions from other sources such as production asymmetry, where the initial number of produced B^+ and B^- mesons differs due to proton–proton collision dynamics and detection asymmetry, where the detector may have different efficiencies for positively and negatively charged particles. These effects must be considered and corrected in order to isolate the true CP-violating asymmetry.

The statistical uncertainty of the asymmetry can be calculated using the formula:

$$\sigma_A = \sqrt{\frac{1 - A^2}{N^+ + N^-}} \tag{3.4}$$

where A is the true asymmetry, and N^+ and N^- are the numbers of B^+ and B^- meson candidates, respectively.

More importantly, in particle physics, the significance of the result is based on the ratio of the measured asymmetry to its statistical uncertainty σ_A. This significance indicates how likely it is that the observed asymmetry is not due to random fluctuations.

$$\text{Significance} = \frac{A}{\sigma_A} \tag{3.5}$$

The table below shows the results obtained in this analysis.

Observable	**Value**	**Uncertainty** σ_A	**Significance** $\frac{A}{\sigma_A}$
Asymmetry A_{global}	0.0370	0.0065	5.7291

Table 3.2: Summary of the global CP asymmetry.

According to standard conventions, a significance greater than 5σ is considered a discovery. It is evident that the result in this analysis confirms the discovery of CP violation.

3.4 Local CP violation

To further investigate CP violation, local CP asymmetries are explored by analyzing the Dalitz plot distribution of the decay products by the calculation of the invariant masses of the hadron pairs $H1\,H2$ and $H1\,H3$. This method is useful for identifying resonances in the two-body subsystems of the three-body decay.

Figure 3-6(a) shows the scatter plot comparing Simulation and LHCb data. It is clear that there are regions with a higher density of points in the data whereas the simulation displays a more uniform distribution within the triangular phase space. This occurs because the decay of the B meson can also proceed via an intermediate resonance. The decay $B^+ \to K^+K^+K^-$ may proceed through the channel $B^+ \to K^+R^0$. Decays involving R^0 have different CP-violation effects as this is effectively a quasi two-body decay. For simplicity, the $R^0 \to K^+K^-$ channel is excluded.

To extract detailed information, The Dalitz plot analysis can be further impose an ordering on these resonances based on their invariant masses. The resonance with the higher mass is labeled R^0_{High} and the one with the lower mass is labeled R^0_{Low}. This sorting allows for clearer separation and better interpretation of the resonance structures in the Dalitz plot as shown the Figure 3-6(b).

Figure 3-6 identifies resonances in the two-body subsystems in two different regions: one around $3.48 \times 10^6\,\mathrm{MeV}^2/c^4$ and another around $11.7 \times 10^6\,\mathrm{MeV}^2/c^4$. These regions correspond to the masses of the D^0 meson ($\sim 1865\,\mathrm{MeV}/c^2$) and the χ_{c0} meson ($\sim 3415\,\mathrm{MeV}/c^2$).

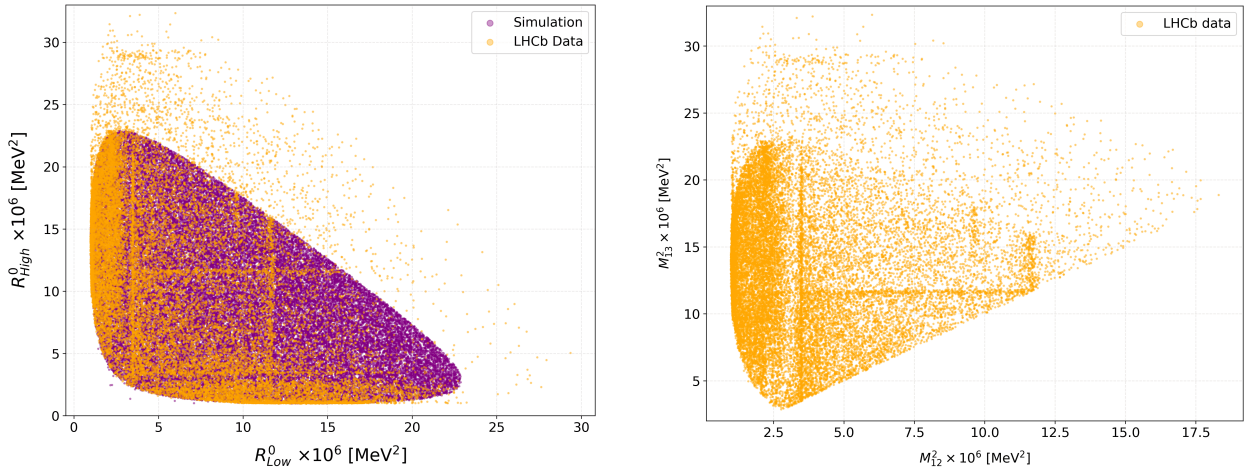

(a) Scatter plot comparing the Simulation and LHCb data distributions

(b) Ordering of the resonances High and Low based on the invariant mass

Figure 3-6: Dalitz plot distribution of the decay products.

To ensure a more precise analysis, the regions corresponding to the D^0 meson and the χ_{c0} meson will be excluded from the subsequent analysis. Figure 3-7 shows the Dalitz plot before and after excluding the regions corresponding to the D^0 and χ_{c0} mesons.

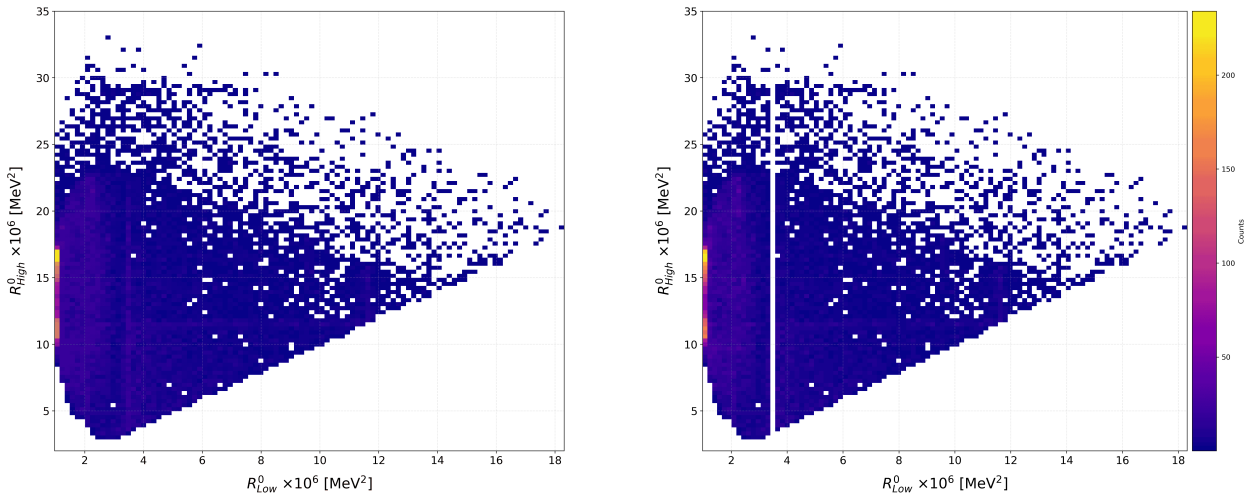

(a) Before excluding regions corresponding to the D^0 and χ_{c0} mesons.

(b) After applying the cuts to remove contributions from D^0 and χ_{c0} resonances.

Figure 3-7: Dalitz plots of the $B^\pm \to K^\pm K^\pm K^\mp$ candidates

Moreover, B^+ and B^- candidates will be analyzed separately in the Dalitz plot to search for local CP asymmetries, as shown in Figure 3-8.

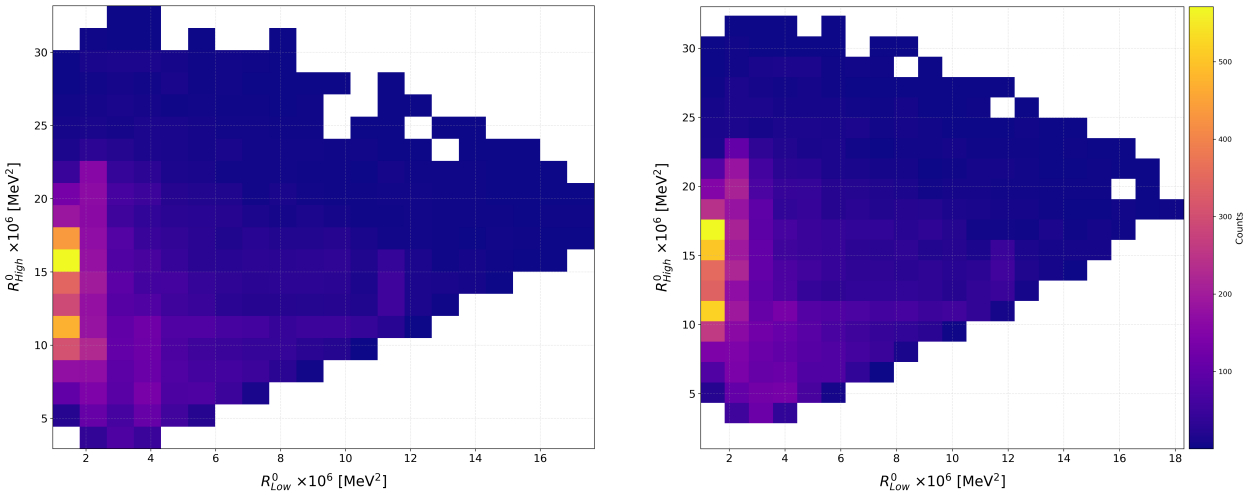

(a) B^+ meson (b) B^- meson

Figure 3-8: Dalitz plots of the selected B^+ and B^- mesons

Figure 3-9 shows a clean region for observing local CP violation. Lower regions of R^0_{Low} and R^0_{High} show significant areas that are potential places to observe CP violation because these regions correspond to mass ranges where asymmetries in particle decay rates are more outstanding. Table 3.3 summarizes the criteria used to select the region of interest.

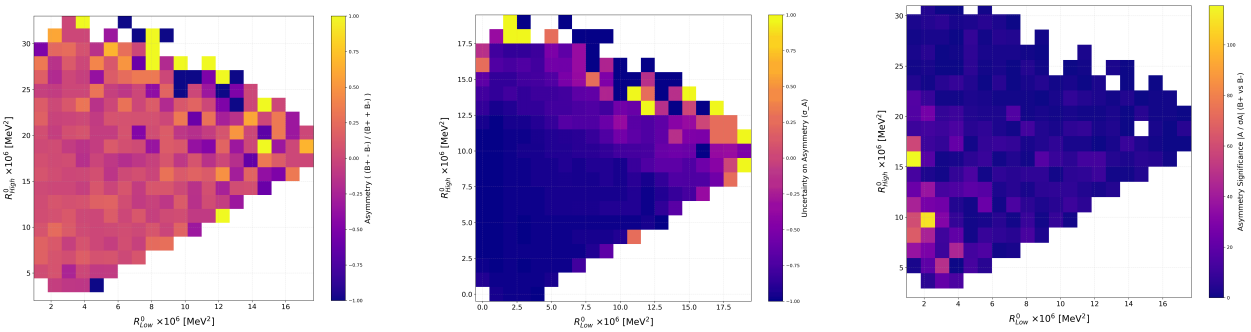

(a) Asymmetry A (b) Statistical uncertainty σ_A (c) Significance $\frac{A}{\sigma_A}$

Figure 3-9: Local CP asymmetry results showing (a) the asymmetry A, (b) the statistical uncertainty σ_A, and (c) the significance $\frac{A}{\sigma_A}$ calculated from the Dalitz plot analysis.

Table 3.3: Selection criteria applied for candidate regions of local CP violation.

Unit: 10^6 [MeV^2]
$R^0_{\text{Low}} < 3 \quad \text{and } 6 < R^0_{\text{High}} < 14 \quad \text{or } 15 < R^0_{\text{High}} < 16$

Following the same procedure used to calculate global asymmetries in Section 3.3, local CP asymmetries are evaluated by comparing event in corresponding bins of the Dalitz plots for B^+ and B^- candidates. Figure 3-9 shows the asymmetry calculated using Equation 3.3, the

statistical uncertainty from Equation 3.4 and the resulting significance according to Equation 3.5. Moreover there are systematic uncertainties due to a production asymmetry between B^+ and B^- mesons as they may not be produced at the same rates. This asymmetry is estimated to be approximately 1%. The table below shows the results obtained for local analysis.

Observable	**Value**	**Uncertainty** σ_A	**Significance** $\frac{A}{\sigma_A}$
Asymmetry A_{local}	0.1238	0.02085	6.767

Table 3.4: Summary of the local CP asymmetry.

Therefore, the invariant mass distribution of B^+ and B^- mesons can be calculated using equation 3.1. The plots shown in Figure 3-10 have peaks at $5282.74 \pm 22.75\,\text{MeV}$ and $5283.73 \pm 21.82\,\text{MeV}$ for B^+ and B^-, respectively.

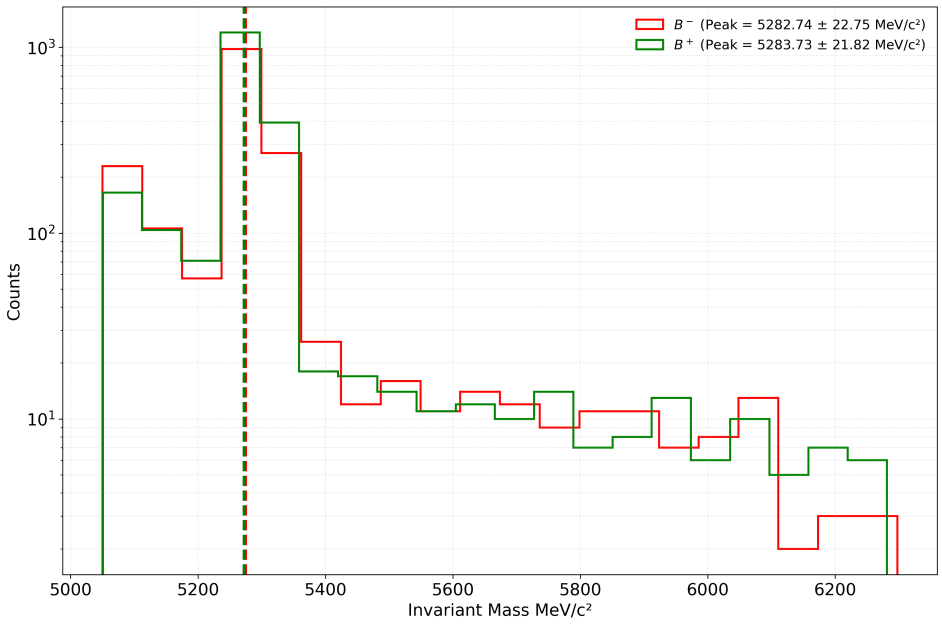

Figure 3-10: Invariant mass distributions of the B^+ and B^- mesons

Chapter 4

Conclusion

The analysis of the decay channels $B^+ \to K^+K^+K$ and $B^- \to K^-K^-K^+$ through both simulation and LHCb experimental data has confirmed the presence of CP violation, both globally and locally. The simulation results closely matched those obtained from the LHCb detector, validating the analysis procedure. The global CP asymmetry was measured to be A = 0.0370 with an uncertainty of ± 0.0065 and significance of $5.73\,\sigma$, satisfying the discovery threshold in particle physics. Additionally, local CP asymmetry identified through Dalitz plot analysis yielded A = 0.1238 with an uncertainty of ± 0.0209 and significance of $6.77\,\sigma$, further strengthening the evidence for CP violation. These results not only support the predictions of the Standard Model but also point toward unexplained asymmetries that may hint at new physics.

Literatures

[1] The Belle Collaboration and K. Abe. Study of charmless b decays to three-kaon final states, 2002.